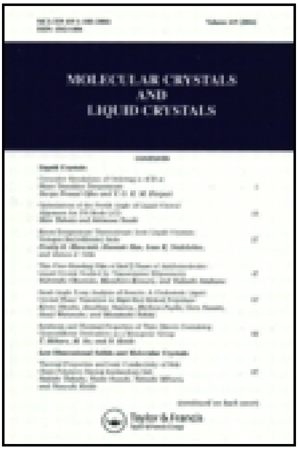

Molecular Crystals and Liquid Crystals Science and Technology. Section A. Molecular Crystals and Liquid Crystals

Publication details, including instructions for authors and subscription information:
http://www.tandfonline.com/loi/gmcl19

Interpretation of Transient Stokes Shift Experiments in Liquid Crystals

Paolo Bartolini [a] , Marilena Ricci [a] , Roberto Righini [a] , Giacomo Saielli [b] , Antonino Polimeno [b] & Pier Luigi Nordio [b]

[a] LENS European Laboratory for Non Linear Spectroscopy, Largo E. Fermi 2, 50125, Firenze, ITALY

[b] Dipartimento di Chimica Fisica Università di Padova, Via Loredan 2, 35131, Padova, ITALY

To cite this article: Paolo Bartolini, Marilena Ricci, Roberto Righini, Giacomo Saielli, Antonino Polimeno & Pier Luigi Nordio (1999): Interpretation of Transient Stokes Shift Experiments in Liquid Crystals, Molecular Crystals and Liquid Crystals Science and Technology. Section A. Molecular Crystals and Liquid Crystals, 336:1, 33-45

To link to this article: http://dx.doi.org/10.1080/10587259908026019

Mol. Cryst. and Liq. Cryst., 1999, Vol. 336, pp. 33-45
Reprints available directly from the publisher
Photocopying permitted by license only

Interpretation of Transient Stokes Shift Experiments in Liquid Crystals

PAOLO BARTOLINI[a], MARILENA RICCI[a], ROBERTO RIGHINI[a], GIACOMO SAIELLI[b], ANTONINO POLIMENO[b]* and PIER LUIGI NORDIO[b]

[a]*LENS European Laboratory for Non Linear Spectroscopy, Largo E. Fermi 2, 50125 Firenze, ITALY and* [b]*Dipartimento di Chimica Fisica Università di Padova, Via Loredan 2, 35131 Padova, ITALY*

We have extensively investigated the effect of the nematic barrier on the transient Stokes shift dynamics of a fluorescent dye with the aid of a stochastic model. A theoretical transient Stokes shift correlation function has been defined and its characteristic decay time has been determined for a wide range of dynamical regimes and dipolar coupling of the solute with the polar environment. Recent experimental data have been reviewed and discussed in relation with the newly available theoretical results.

Keywords: transient Stokes shift; solvatochromic dynamics; stochastic models

INTRODUCTION

Photoinduced solvation processes are widely investigated to extract information on the orientational dynamics of condensed phases. The fluorescence transient Stokes shift (TSS) of a dye dissolved in a polar solvent is a clear manifestation of the process of solvent reorganization. In this experiment, a short laser pulse excite the dye from the ground state S_0 to the

---

* Corresponding author

first singlet state S_1. Usually the transition is accompanied by a change in the permanent dipole moment $\underline{\mu}$ of the solute, therefore, after the excitation, the solvent starts to readjust towards the new equilibrium state. This process has the effect of lowering the energy of the excited state and shifting the fluorescence band to the red. An empirical correlation function, which describes the relaxation process can be defined as

$$C(t) = \frac{\omega(t) - \omega(\infty)}{\omega(0) - \omega(\infty)} \tag{1}$$

where $\omega(0)$, $\omega(t)$ and $\omega(\infty)$ are the maximum of the frequency of the fluorescence band at time 0, t, and ∞ respectively. In this communication we present some recent theoretical results on the effect of the presence of a nematic barrier on the Transient Stokes shift (TSS) dynamics and we further discuss recent experimental data[1].

EXPERIMENTAL SECTION

Coumarin 503, C503 hereafter, and ZLI 1167 were purchased, respectively, from Exciton Dye laser and Merck and they do not show fluorescent impurities. A solution of C503 in ZlI 1167 was prepared at the concentration of *ca.* 10^{-4} M and put into a 2 mm quarts cell. Absorption spectra were recordered with a Perkin Elmer - Lambda 6 Spectrometer and fluorescence spectra with a Perkin Elmer LS50 Spectrofluorimeter.

Experimental set-up

The experimental set up has been already described elsewhere[2]. The light source was a tunable dye laser pumped by the second harmonic of a modelocked Nd-Yag laser, having a repetition rate of 74 MHz. The dye laser wavelength was fixed at 684 nm and the pulse width was *ca.* 1.5 ps. At the laser output a pockel cell reduced the frequency repetion rate of the pulse to 164 kHz, in order to follow the whole ground state recovery of the probe molecule after excitation. The excitation beam was duplicated by BBO crystal (the wavelength was at the left side of the absorption band of C503) and focused onto the sample. A forward collection geometry was used with a slight tilt angle to separate the excitation beam from the emitted fluorescence.

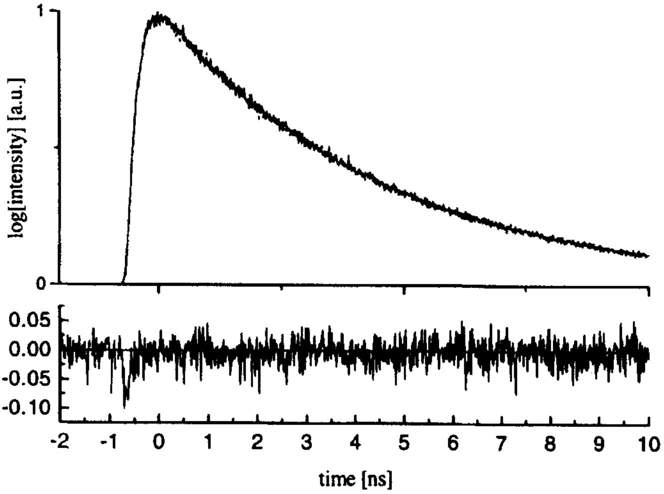

FIGURE 1: normalised fluorescence decays I_{VV} (solid) and I_{VH} (dashed), see the text for the discussion. The two curves are almost superimposed. On the bottom panel we show the difference between the two curves.

The experimental decays were collected in the nematic and isotropic phase of sample, increasing the temperature in the ordered phase from 311.5 K to 353 K and at three temperatures in the isotropic phase up to 373 K (the clearing point was Tc= 356 K). The measurements of fluorescence decay time in the isotropic phase were performed at the "magic angle" experimental configuration (vertically polarized excitation beam and 54.7° polarized fluorescence collection), while in the nematic phase the sample was not macroscopically oriented, so it was consisting of a isotropic distribution of oriented micro-domains. The birefringence of micro-domains turned out to be a very efficient depolarizing mechanism, yielding any experimental geometries equivalent to the "magic angle" configuration. In order to confirm this ipothesis, we performed measurements of the fluorescence decay in I_{VV} and I_{VH} (vertical excitation and, respectively, vertical and horizontal collection).

As we can see in the Fig.1, the two decay curves are identical: a deconvolution using a biexponential function, gave, for both curves, a reduced $\chi^2 \leq 1.10$ and the same fitting parameters. This is evidence that orientational dynamics of the emitting molecule does not contribute to the observed fluorescence emission.

Results

In order to obtain fluorescence intensity as a function of wavelength and time, we follow the spectral reconstruction procedure[3]. We have collected fluorescence decays with steps of 5 nm around the maximun and 10 nm around red and blue tails, spanning the stationary fluorescence emission band from 415 nm to 525 nm. The decay curves were then deconvoluted by means of sum of exponentials as model function to represent analitically the decay itself, giving a reduced $\chi^2 \leq 1.10$. All traces present a long decay, attributed to the fluorescence lifetime, while at short time it is visible the effect of Stokes shift as a fast additional decay depending on the emission wavelength[1]. Each decay was then normalized according to the following expression:

$$I(2\pi / \lambda, t) = I(\nu, t) \propto \lambda^2 F(\lambda, t) I_0(\lambda) / \int_0^{\infty} F(\lambda, t') dt' \qquad (2)$$

where $F(\lambda,t)$ is the model function representing the decay curve at wavelength λ and $I_0(\lambda,t)$ is the static fluorescence spectrum. $I(\nu,t)$ can be used to obtain time resolved spectra plotting $I(\nu)$ for a fixed time. Each spectrum is then fitted by log-norm function that is asymmetric band shape curve defined by four parameters, bandwidth, skewness, peak position and amplitude, which reduces to a Gaussian curve in the limit of null skewness. Finally the Stokes shift correlation function is calculated as function of $\omega(t)$, $\omega(\infty)$ and $\omega(0)$ by means of Eq. 1.

The analysis of transient Stokes shift decay curves reveals a clear biexponential behaviour. The values of the slow (τ_S) and fast (τ_F) decay constant of the TSS curves are shown in Tab. 1. The two time constants have approximately the same amplitude and are well separated. The faster component of the dynamics is detectable up to 331.5 K, and it becomes shorter than instrumental resolution (100 ps) about this temperature. On the contrary, the slow dynamics can be monitored in all the nematic range and up to 20 K above the clearing point.

It is worth noticing that the variation of the TSS correlation time at the nematic-isotropic transition is quite small if compared with the slowing down effect of the dielectric relaxation of common nematics. This feature will be further investigated in the next section.

TABLE 1: The values of the slow (τ_S) and fast (τ_F) decays of the TSS function (Eq. 1) are reported vs temperature. The last three time constants are referred to the isotropic phase (T_c =356K). Statistical error is about 10%.

T/K	τ_1/ns	τ_2/ns
311.5	1.666	0.392
317.5	1.430	0.181
323	0.955	0.202
331.5	0.748	0.137
338.5	0.538	-
345.5	0.505	-
349.5	0.504	-
354.5	0.425	-
358	0.309	-
363	0.328	-
373	0.230	-

THEORETICAL SECTION

The Sthocastic Model

The stochastic model has been already described in Ref. [1]. We recall here some basic concepts. The system is made of a rotating point dipole inside a spherical Onsager cavity, surrounded by a homogeneous polar medium. The equilibrium distribution is calculated with respect to the set of coordinates $\underline{q}\equiv(\underline{\Omega},\underline{X})$. $\underline{\Omega}$ represents the three Euler angles defining the orientation of the molecular frame (MF) with respect to the laboratory frame (LF). We assume the permanent dipole moment to be aligned along the z axis of the MF. $\underline{X}$ is the vector representing the solvent stochastic reaction field, which is coupled with the solute dipole. The adiabatic energy surface for the excited state is defined, neglecting constant terms, as:

$$E = -\gamma P_2(\cos\beta) - \underline{\mu} \cdot \underline{X} + \frac{1}{2}\Xi^2 X^2 \tag{3}$$

The three terms in Eq. 3 represents respectively the mean field potential of a nematic phase, in its simpler form^4, the interaction energy between the solute and the solvent reaction field and the fluctuations of the reaction field itself, which is assumed to be confined in an harmonic minimum. γ is the strength of the mean field potential; the coefficient Ξ is defined by the following relation:

$$\frac{1}{\Xi} = \frac{1}{\Xi_0} - \frac{1}{\Xi_\infty} = \frac{1}{4\pi\,\epsilon_0\,a^3}\left(\frac{\varepsilon_0 - 1}{\varepsilon_0 + 1/2} - \frac{\varepsilon_\infty - 1}{\varepsilon_\infty + 1/2}\right) \tag{4}$$

where a is the Onsager cavity radius, ϵ_0 is the vacuum permittivity and ε_0 and ε_∞ are the static and optical dielectric permittivity of the medium.

Both coordinates, $\underline{\Omega}$ and $\underline{X}$, are assumed to be diffusive, as expected for condensed fluid phases. The time evolution of the distribution of probability $P(\underline{\Omega},\underline{X},t)$ is then described by the following Smoluchowski equation:

$$\frac{\partial}{\partial t} P(\underline{\Omega},\underline{X},t) = -\hat{\Gamma} P(\underline{\Omega},\underline{X},t) \tag{5}$$

where the time evolution operator $\hat{\Gamma}$ is defined as:

$$\hat{\Gamma} = -\underline{\hat{M}}\,\underline{\underline{D}}_R P_{eq} \underline{\hat{M}} P_{eq}^{-1} - \underline{\hat{\nabla}}\,\underline{\underline{D}}_S P_{eq} \underline{\hat{\nabla}} P_{eq}^{-1} \tag{6}$$

and P_{eq} is the equilibrium distribution given by the Boltzmann distribution:

$$P_{eq} \equiv P_{eq}(\underline{\Omega}, \underline{X}) = \frac{\exp[-E(\underline{\Omega}, \underline{X}) / k_B T]}{\langle \exp[-E(\underline{\Omega}, \underline{X}) / k_B T] \rangle} \tag{7}$$

In Eq. $\hat{\underline{M}}$ is the infinitesimal rotation operator for rigid body, acting on $\underline{\Omega}$ and $\underline{\underline{D}}_R$ is the rotational diffusion tensor of the solute; $\hat{\underline{\nabla}}$ is the gradient operator with respect to the solvent reaction field coordinate $\underline{X}$ and $\underline{\underline{D}}_S$ is the corresponding diffusion tensor. The transient Stokes shift observable has no dependence from the third Euler angle, defining the spinning motion of the solute molecule about its *z* axis, so that we can neglect such a motion using a reduced infinitesimal rotation operator $\hat{\underline{\mathfrak{m}}}$ describing the motion of a vector instead of a rigid body. Since the *x* and *y* axis of the MF are equivalent, only the perpendicular component (tumbling motion) of the rotational diffusion tensor enter in the definition of the time evolution operator. The diffusion tensor for the solvent reaction field has a spherical symmetry when we describe the isotropic phase, while it has a cilindical simmetry in the nematic phase, with two independent components, $D_S^{\perp}$ and $D_S^{\parallel}$. Finally we can write the time evolution operator as:

$$\hat{\Gamma} = -D_R^{\perp} \hat{\underline{\mathfrak{m}}} P_{eq} \hat{\underline{\mathfrak{m}}} P_{eq}^{-1} - \hat{\underline{\nabla}} \underline{\underline{D}}_S P_{eq} \hat{\underline{\nabla}} P_{eq}^{-1} \tag{8}$$

To complete the definition of the model we need to define a theoretical expression for the TSS observable. It is possible to show[1] that the normalized response function of Eq. 1 corresponds to the following autocorrelation function:

$$C(t) = \langle \underline{z} \cdot \underline{X} | \exp(-\hat{\Gamma} t) | \underline{z} \cdot \underline{X} P_{eq} \rangle - \mu^2 \tag{9}$$

where z is the unitary vector defining the orientation of the dipole moment in the excited state, while μ is its modulus.

The TSS observable is clearly defined as the autocorrelation function of the rescaled interaction energy between the solute dipole and the solvent reaction field, a definition which agrees with the intuitive picture of TSS probed by the shift in time of the fluorescence band on an energy axis.

Results and Discussion

In a previous work[1] we have attempted to reproduce the dynamical behaviour of the experimental system over the complete range of temperatures investigated. In a following contribution[5], an asymptotic treatment, valid in limiting cases of large anisotropy of diffusion between the two sets of variables, has been presented. Up to now a complete investigation of the behaviour of the TSS observable *at* the isotropic-nematic transition for all the dynamical regimes and range of dipolar coupling is still missing and will be discussed here.

It is well known that orientational correlation functions of first and second rank are affected by the presence of a nematic barrier in a very different way: first rank observables are strongly slowered in the nematic phase because the dominant dynamical process which they describe is the barrier crossing between the two equivalent minima of the nematic potential, which is an activated process. On the contrary, second rank observables become usually slightly faster in the nematic phase, because they represents the equilibration process inside the minima of the nematic potential, so that they are influenced mainly by the curvature of the well, which is increasing at the transition from the isotropic to the nematic phase. This behaviour can be interpreted in a very *naif* way considering the parity of the observables and of the mean field potential: a first rank observable behaves as $\cos\beta$, taking different values in the two equivalent minima of the nematic potential. More precisely it is positive for values of the angle β close to zero and negative when β is around π. As a result, a relaxation of the observable cosβ, which means a complete exploration of its phase space, implies the crossing of the nematic barrier. On the contrary, second rank observables behaves like $\cos^2\beta$, which takes the same values in both minima, so that the equilibrium is reached by simply exploring one of the two equivalent minima of the mean field potential.

Transient Stokes shift observable has been defined as a scalar product between two vectors, namely the solute dipole moment $\underline{\mu}$ of the excited state and the solvent reaction field $\underline{X}$. It is therefore a scalar quantity. This obvious observation is more than a mere curiosity because it means that TSS observable should be independent on a rotation of the reference frame, thus it behaves as a zeroth rank tensor. From this point of view we expect TSS to be quite independent from the presence of a nematic barrier, and this is, actually, the result of the experiments discussed previously. However, the effective time dependence of the observable depends on the dynamical regime under investigation, even though, for system of physical interest, the model always predicts TSS to be only slightly affected by the nematic-isotropic transition.

To characterize the behaviour of the TSS at the transition we have calculated the average correlation time of the TSS correlation function in the isotropic phase (parameter γ of Eq. set to zero), τ_I, and the corresponding time for the nematic phase (γ=2.0 k_BT), τ_N. The value γ=2.0 k_BT is quite close to the value predicted by the Maier-Saupe theory of nematics at the clearing point. The calculations have been done for different values of the anisotropy of diffusion $D_R^{\perp} / D_S^{iso}$, where D_S^{iso} is the solvent polarisation diffusion coefficient in the isotropic phase. In the nematic phase the ratio between the two components of the tensor $\underline{D}_S$ have been taken equal to 2.0 and with an average value corresponding to D_S^{iso}. We remind that, although the difference between the longitudinal and transverse dielectric relaxation time, in the nematic phase, can be of a factor of ten, at the transition, the ratio between the diagonal components of the solvent diffusion tensor is much closer to unity, due to the scaling with the dielectric permittivity constants:

$$D_S^{\parallel,\perp} = \frac{\varepsilon_0^{\parallel,\perp}}{\varepsilon_\infty^{\parallel,\perp}} \cdot \frac{1}{\tau_D^{\parallel,\perp}} \tag{10}$$

where $\varepsilon_{0,\infty}^{\parallel,\perp}$ are the parallel and perpendicular components of the static and optic dielectric permittivity tensor respectively, and τ_D is the dielectric relaxation time.

As we see from Eqs. 3 and 4, the strenght of the dipolar coupling depends on several experimental parameters, namely the radius of the Onsager cavity, the modulus of the dipole moment, the solvent polarity. It is, therefore, convenient to define a rescaled dipole as $|\underline{\mu}| \Rightarrow (k_B T)^{1/2} \Xi |\underline{\mu}|$.

The rescaled dipole moment is the only parameter that we need to specify in the model, in addition to the diffusion coefficients and the nematic barrier parameter γ. It should be regarded as a measure of the strenght of the dipolar coupling more than the value of the solute dipole, since the polarity of the solvent and the radius of the Onsager cavity enter in the definition through the parameter Ξ.

In Fig. 2 we show the calculated ratio of the average correlation times for TSS in nematic and isotropic phase, as described previously, as a function of both the anisotropy of diffusion and strength of the dipolar coupling. If the ratio is close to unity it means that the effect of the nematic barrier on TSS dynamics is negligible. This results show that a significant effect is present only in the case of "slow solvent" and small dipolar coupling. In all the other cases we can see that the change in the correlation time at the transition are very small. However, the physical meaning of the "slow solvent" case should not be overestimated: firstly, a dynamical regime in which the solvent diffusion coefficient is more than 10 times smaller that the solute orientational diffusion coefficient is quite uncommon. Secondly, a small value of the dipolar coupling is required and in this limit the TSS itself is small.

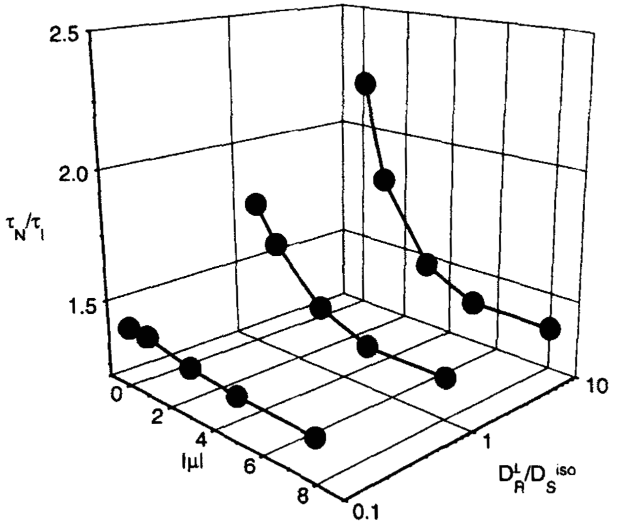

FIGURE 2: ratio between the TSS correlation time in nematic and isotropic phase as a function of the anisotropy of diffusion and strnght of the dipolar coupling.

Finally we note that the correlation time for a first rank observable, calculated for same dynamical regimes, show an increase, on going in the nematic phase, of about a factor of five.

CONCLUSIONS

In this comunication we have shown how the presence of a nematic barrier in the orientational potential affects the TSS dynamics. A range of dynamical regimes has been investigated. The results show that TSS observable is nearly independent from the presence of a nematic barrier in all the conditions of physical interest. Experimental results of TSS of the dye Cumarin 503 in the mesogenic mixture ZLI 1167 agree with the theoretical prediction and can be interpreted in the framework of the stochastic model.

Acknowledgements

This work has been supported by the EC TMR contract FMRX-CT97-0121 and by the Italian Ministry for Universities and Scientific and Technological Research.

References

[1] G. Saielli, A. Polimeno, P.L. Nordio, P. Bartolini, M. Ricci and R. Righini, *J. Chem. Soc. Faraday Trans.*, **94,** 121 (1998).
[2] D. Paparo, L. Marucci, G. Abbate, E. Santamato, P. Bartolini, R. Torre, *Mol. Cryst. Liq. cryst.*, 1996, 282, 461.
[3] D.B. Siano, D.E. Metzler, *J. Chem. Phys.*, **51,** 1856 (1969).
[4] G. Meier and A. Saupe, *Mol. Cryst.*, **1,** 515 (1966).
[5] A. Polimeno, G. Saielli and P.L. Nordio, *Chem. Phys.*, in press.